Transp Porous Med (2008) 73:57–74
DOI 10.1007/s11242-007-9160-1

CO_2 Injection into Saline Carbonate Aquifer Formations II: Comparison of Numerical Simulations to Experiments

Omer Izgec · Birol Demiral · Henri Bertin · Serhat Akin

Received: 19 July 2005 / Accepted: 14 August 2007 / Published online: 25 September 2007

Abstract Sequestration of carbon dioxide in geological formations is an alternative way of managing extra carbon. Although there are a number of mathematical modeling studies related to this subject, experimental studies are limited and most studies focus on injection into sandstone reservoirs as opposed to carbonate ones. This study describes a fully coupled geochemical compositional equation-of-state compositional simulator (STARS) for the simulation of CO_2 storage in saline aquifers. STARS models physical phenomena including (1) thermodynamics of sub- and supercritical CO_2, and PVT properties of mixtures of CO_2 with other fluids, including (saline) water; (2) fluid mechanics of single and multiphase flow when CO_2 is injected into aquifers; (3) coupled hydrochemical effects due to interactions between CO_2, reservoir fluids, and primary mineral assemblages; and (4) coupled hydromechanical effects, such as porosity and permeability change due to the aforementioned blocking of pores by carbonate particles and increased fluid pressures from CO_2 injection. Matching computerized tomography monitored laboratory experiments showed the uses of the simulation model. In the simulations dissolution and deposition of calcite as well as adsorption of CO_2 that showed the migration of CO_2 and the dissociation of CO_2 into HCO_3 and its subsequent conversion into carbonate minerals were considered. It was observed that solubility and hydrodynamic storage of CO_2 is larger compared to mineral trapping.

Keywords CO_2 injection · Aquifer · Calcite deposition · Permeability and porosity alteration · Numerical model

O. Izgec · S. Akin (✉)
Petroleum and Natural Gas Engineering Department, Middle East Technical University, Inonu Bulvari, Ankara 06531, Turkey
e-mail: serhat@metu.edu.tr

B. Demiral
Geoscience and Petroleum Engineering Department, Universiti Teknologi Petronas, Bandar Seri Iskandar, Tronoh, Perak 31750, Malaysia

H. Bertin
Laboratoire TREFLE, Esplanade des Arts et Métiers, Talence Cedex 33405, France

Nomenclature

k_f	Instantaneous absolute permeability
k_0	Initial absolute permeability
c	Kozeny–Carman-power
s_{ki}	Reactant stoichiometric coefficient of reaction k
s'_{ki}	Product stoichiometric coefficient of reaction k
s_w	Irreducible water saturation
p_d	Entry pressure, MPa
rk	Rate of reaction k
rrk	Constant part of rk
C_i	Concentration of component i in void volume (ppm)
E_{ak}	Temperature dependence of rk
H_{rk}	Reaction enthalpy
R	Gas constant ($\mathrm{Pa \cdot m^3/mol\text{-}K}$)
T	Temperature (K)
λ	Pore-size distribution index of Brooks–Corey model
ϕ	Instantaneous effective porosity
ϕ_0	Initial effective porosity
φ_f	Fraction of void porosity occupied by fluids
φ_s	Fraction of void porosity occupied by solid particles

1 Introduction

Injection of CO_2 into aquifers results in variety of strongly coupled physical and chemical process as multiphase flow, dissolution-deposition kinetics, solute transport, hydrodynamic instabilities due to displacement of less viscous CO_2 with more viscous brine (viscous fingering), capillary effects and upward movement of CO_2 due to gravity (gravity override) (Reichle et al. 1999). Reactions among the formation rock, the aquifer fluid and CO_2 may lead to change in the formation permeability and the effective porosity, thus the storage capacity of the formation.

Through the injection of CO_2 in carbonated deep saline aquifers, some changes in rock properties are expected. Change in the rock permeability and effective porosity result from dissolution of rock minerals, transportation and later precipitation of them. Continuous dissolution of reactant minerals alters the concentration of aquifer fluid, thus in later times leading to precipitation of product phases. While dissolution of rock minerals increases the formation permeability, precipitation of those minerals leads to decrease in the formation permeability and the effective porosity (Lichtner 1996; Xu et al. 2004; Izgec et al. 2007).

At the CO_2 front where CO_2 is dissolved in water, minerals such as calcite may dissolve readily, leading to an increase in permeability and porosity along the flow channel. This leads to a higher flow rate and increased dissolution, forming what is known as wormholes. It is also known that from the various field applications of enhanced oil recovery that CO_2 has been known to reduce injectivity in some cases but to increase permeability near injection wells in others, such as in carbonate reservoirs.

For a carbonate system kinetically controlled reactions could be defined as (Omole and Osaba 1983; Snoeyink and Jenkins 1980):

$$H_2O + CO_2 + CaCO_3 \leftrightarrow Ca(HCO_3)_2 \tag{1}$$

In general, atmospheric or subsurface CO_2 dissolves in water and generates a week carbonic acid, which subsequently dissociates into HCO_3^- and CO_3^- according to reaction steps given

as:

$$CO_{2(gas)} \leftrightarrow CO_{2(aq)} \tag{2}$$

$$CO_{2(aq)} + H_2O \leftrightarrow H_2CO_{3(aq)} \tag{3}$$

$$H_2CO_{3(aq)} \leftrightarrow HCO_3^- + H^+ \tag{4}$$

$$HCO_3^- \leftrightarrow CO_3^{2-} + H^+ \tag{5}$$

The dissolved bicarbonate species react with divalent cations to precipitate carbonate minerals. Formation of Ca, Mg, and Fe(II) carbonates are expected to be the primary means by which CO_2 is immobilized (Gunter et al. 1997).

$$HCO_3^- + Ca^{2+} \leftrightarrow CaCO_3 + H^+ \tag{6}$$

$$HCO_3^- + Mg^{2+} \leftrightarrow MgCO_3 + H^+ \tag{7}$$

$$HCO_3^- + Fe^{2+} \leftrightarrow FeCO_3 + H^+ \tag{8}$$

Mechanisms by which a precipitate reduces permeability include deposition of the carbonate particles precipitated from the saturated solution on the pore walls due to attractive forces between the particles and the surfaces of the pores, individual particles blocking pore throats, and several particles bridging across a pore throat (Pruess and Xu 2001). In a carbonate formation major cause of reduction in rock properties is precipitation of $Ca(HCO_3)_2$ and NaCl. Pressure drop through the flow paths affects the precipitation rate, thus leads to variations in rock properties by changing the solubility of substances. Assuming there is Darcian flow in the porous media, it can be said that there is a linear relationship between the pressure drop and the axial distance in the direction of flow. Considering this relationship and solute transport concept, it should be expected that permeability increases in near well bore region and then gradually decreases through the flow direction (Omole and Osaba 1983). In the case of multiphase flow and/or heterogeneous and fractured formations, dramatic deviations from the linear pressure decrease are reported (Matthai and Belayneh 2004). This, in turn may affect the permeability alteration trends. It is previously reported that permeability decline caused by only calcite deposition in the porous bed can reach to 90% of the initial permeability, depending on solution composition, initial permeability, temperature, and flow rate and solution injection period (Moghadasi et al. 2005). On the other hand, some researchers (Omole and Osaba 1983) reported increase in the permeability of dolomite cores by 3.5–5% after similar CO_2 treatments while reduction in permeability was observed in other experiments. Those results suggest that the process strongly depends on the distribution of the rock minerals.

As discussed-above, injection of CO_2 in geologic formations may give rise to a number of physical and chemical phenomena, such as miscible or immiscible displacement of native fluids, dissolution of injected fluids into reservoir fluids, changes in effective stress with associated porosity and permeability change and the possibility of inducing seismic activity, chemical interactions between fluids and solids, and nonisothermal effects. Johnson et al. (2001) simulated the large scale injection of CO_2 currently being produced at Statoil's Sleipner facility in the Norwegian sector of the North Sea (Korbol and Kaddour 1995). They analyzed the coupled processes and mechanisms that lead to structural, solubility, and mineral trapping, and quantified the relative effectiveness of the distinct sequestration processes

as a function of key reservoir properties. White et al. (2001) applied reactive chemical transport modeling to simulate mineral sequestration of CO_2 in saline reservoirs underlying the Colorado Plateau. McPherson and Lichtner (2001) used a mathematical sedimentary basin model, including multiphase flow of CO_2, groundwater, and brine, to evaluate resident times in possible aquifer storage sites and migration patterns and rates away from such sites in the Powder River Basin of Wyoming. Numerical simulation of CO_2 disposal in aquifers has also been studied by Doughty and Pruess (2004), Xu et al. (2004), Allen et al. (2005), Kumar et al. (2005), and Lagneau et al. (2005). In these studies, local equilibrium is assumed to govern the distribution of aqueous chemical species. A critical comparison of simulation codes that could be used to model injection of CO_2 in geologic formations was presented by Pruess et al. (2002). They concluded that a considerable number of numerical simulation codes (i.e., CMG's GEM, Geoquest's Eclipse, TOUGH2, etc.) were capable of simulating, in realistic, quantitative detail, the important flow and transport processes that would accompany geologic sequestration; however, the hydromechanical test problem was solved by only one code (TOUGH-FLAC).

In this study, we propose an alternative numerical model developed using CMG's STARS that considers physical phenomena including (1) thermodynamics of sub- and supercritical CO_2, and PVT properties of mixtures of CO_2 with other fluids, including (saline) water; (2) fluid mechanics of single and multiphase flow when CO_2 is injected into aquifers; (3) coupled hydrochemical effects due to interactions between CO_2, reservoir fluids, and primary mineral assemblages; and (4) coupled hydromechanical effects, such as porosity and permeability change due to the aforementioned blocking of pores by carbonate particles and increased fluid pressures from CO_2 injection. Unlike the aforementioned numerical simulation studies permeability change as a result of dissolution and deposition of the carbonate particles precipitated from the saturated solution on the pore walls, individual particles blocking pore throats, and several particles bridging across a pore throat and adsorption of CO_2 is considered in the developed numerical model. The reaction model's heterogeneous mass transfer (source and sink) terms were applied to the nonequilibrium capture and release of calcite particles as well as salt particles by the porous rock. First details of the model will be given. Then calibration of the model using CT monitored experiments will be introduced. Sensitivity analyses of deposition and dissolution reactions, as well as other important simulation parameters will be discussed.

2 Numerical Modeling Approach

2.1 Main Features

CMG's STARS (CMG 2003) compositional advanced processes and thermal finite difference reservoir simulator is capable of simulating many types of chemical additive processes such as surfactant and polymer injection, using cartesian or cylindrical grid and porosity models (single porosity or double porosity) in both laboratory and field scale. STARS is previously used to simulate several processes including CO_2 injection into coal bed methane reservoirs (Law et al. 2001), modeling phase behavior including the effect of pressure and temperature on asphaltene precipitation during primary production (Kohse et al. 2000) and fully implicit thermal simulation for multicomponent fluid flows (Siu et al. 1990). Law et al. (2001) stated that the predicted CH_4 production rates and compositions in the produced gas streams predictions by STARS and ECLIPSE were in general agreement for pure CO_2 injection into a

coal bed methane reservoir. This indicates that STARS has a very similar performance even though it uses a very different modeling approach compared to ECLIPSE.

One conservation equation for each chemical component for which a separate accounting is desired, and two separate phases (water and gas) along with equations describing phase equilibrium between phases are used to model injection of CO_2. There exists a set of these equations for each region of interest, which is usually a discretized grid block. Lastly, there is an equation describing the operating condition of each injection and production well. An implicit time weighing scheme is used for the individual components of the model consisting of flow, transport, and geochemical reaction. A fully implicit approach, which simultaneously solves the transport and the reaction equations was used. No flow boundary conditions are used. CO_2 was defined as real gas and its solubility in water is taken to be proportional to CO_2 partial pressures at pressures of a few bars, but increases only very weakly with pressure beyond 100 bars (Spycher et al. 2003). A Henry's law formulation with fugacity correction was used. Supercritical dilute aqueous CO_2 thermodynamical properties adapted from Sengers et al. (1992) are input in a tabular fashion. Water viscosity and density is taken to be function of temperature and salinity only. The dissolution and deposition reactions given by Eq. 1 through 5 are implemented and treated separately. The reaction model's heterogeneous mass transfer (source and sink) terms were applied to the nonequilibrium capture and release of calcite particles as well as salt particles by the porous rock. These particles captured by the porous medium can cause permeability reductions (blockage) in a manner similar to equilibrium mass transfer to the rock (adsorption). The reaction source/sink term is given as:

$$V \sum_{k=1}^{nr} \left(s'_{ki} - s_{ki}\right) \bullet rk \tag{9}$$

where s_{ki} and s'_{ki} represent the reactant and product stoichiometric coefficients of reaction k. Equation 9 proceeds at the rate of rk moles per day per reservoir volume. This relationship has one degree of freedom, which is a proportionality factor. The quantities s_{ki} and s'_{ki} can be multiplied by an arbitrary factor "a", but rk must be divided by "a" so that the source/sink terms remain. Usually the factor "a" is chosen such that $s_{ki} = 1$ for the main reacting component. The kinetic model determines the speed of reaction rk. The general expression is given by:

$$rk = r_{rk} \cdot \exp\left(\frac{-E_{ak}}{RT}\right) \cdot \prod_{i=1}^{nc} C_i \tag{10}$$

where r_{rk} is reaction rate constant that specifies the frequency of the reaction, E_{ak} is the activation energy; E_{ak} that determines the temperature dependence of reaction rate, rk. While the enthalpies of reaction can be characterized between well-defined limits and can even be calculated from first principles, the observed activation energies can vary dramatically. This is because certain components in the rock surface may act as catalysts. The concentration factor for reacting component i is given as follows:

$$C_i = \varphi_f \cdot \rho_j \cdot s_j \cdot x_{ji} \tag{11}$$

where j is the phase in which component i is reacting, and x_{ji} represents water or gas mole fractions, φ_f is fluid porosity, ρ_j is density, and s_j is saturation. Concentration factor for the solid component is given by

$$C_i = \varphi_v c_i \tag{12}$$

where φ_v is void porosity (ratio of void volume to gross volume) and c_i is the concentration of component i in void volume. The void porosity can be occupied by fluids (represented by fluid porosity, φ_f) and the deposited calcite particles (represented by solid porosity, φ_s). Fluid porosity and void porosity is related with the following relationship.

$$\varphi_f = \varphi_v = \left[1 - F_{\text{fluid}} - \sum_i \left(\frac{c_i}{\rho_{si}}\right)\right] \tag{13}$$

where F_{fluid} is the fraction of void volume occupied by fluid components. It then requires that the permeability depends upon reaction rate constants, to account for the changes in capture efficiency as the calcite particle size to pore throat size ratio changes. To specify the dependence of permeability on chemical reactions and nonequilibrium mass transfer an effective permeability reaction rate scaling factor table (i.e., Table 2) was used. Once porosity as a function of time is calculated permeability is adjusted accordingly. Thus, permeability change was controlled by reaction frequencies (1/min-kPa) of the dissolution and deposition reactions and Kozeny–Carman coefficient (c) given by Eq. 14 (CMG 2003).

$$k_f = k_0 \left(\frac{\phi}{\phi_0}\right)^c \left(\frac{1-\phi_0}{1-\phi}\right)^2 \tag{14}$$

The rate of propagation of in situ created calcite particles are strongly affected by their interaction with the rock matrix. These interactions can be chemical (e.g., ion exchange) or mechanical (e.g., blockage) or some combination of mechanisms. The capture levels can depend on fluid concentrations, temperature and rock type (e.g., permeability). A phenomenological description of these phenomena, wherein a set of constant temperature adsorption isotherms (adsorption level as a function of fluid composition) are input, is adapted. These isotherms can be either in tabular form or in terms of the well-known Langmuir isotherm correlation.

$$AD = \frac{A \cdot z}{1 + Bz} \tag{15}$$

Where z is some fluid component composition, A and B are generally temperature dependent Langmuir constants. The maximum adsorption level associated with this formula is A/B. Permeability alteration often accompanies adsorption (especially if adsorption is of mechanical, blockage type). The simulator accounts for this via region dependent resistance factors (*RRF*) which allow correlation of local permeability with local adsorption levels. It is assumed that only single-phase flow paths are altered. Thus for example, the gas phase permeability reduction factor is defined as

$$RKG = 1 + (RRF - 1)^* AD/ADMAXT \tag{16}$$

RKG varies between 1.0 and a maximum of *RRF* as adsorption level increases. The mobility of the gas phase is divided by *RKG*, thus accounting for blockage. Ideally, not only the adsorption maximum but the rate of increase of adsorption with fluid composition should be known in order to fit the two Langmuir parameters A and B. If this is not reported, as is often the case, one must use the fluid composition at the adsorption maximum to indirectly determine this second factor.

From the aforementioned discussion, critical simulation parameters can be summarized as follows:

1. Dissolution and deposition reaction frequencies;
2. Kozeny–Carman coefficient;

3. Reaction rate scaling factor;
4. Blockage effect of particles;
5. Adsorption rate of CO_2; and
6. Initial concentration of solid phase carbonate and aqueous phase bicarbonate, aqueous phase sodium bromide particles.

For a typical problem cumulative mass balance errors at the ending time were less than 1% for all components. In order to achieve this level of accuracy and to prevent large material balance errors due to insufficient accuracy of iterative matrix solution, a precision parameter that is the ratio by which the mean equation residual must be reduced from its initial value before the solution is accepted or used. When used with an automatic time-step cutting control algorithm this method ensured accurate solutions with 10–15 Newton cycles per time-step. As the size of a problem increases, the relative amount of time spent in the various STARS component routines will change. The time spent in the EOS routine increases roughly, linearly with the size of the problem (number of equations solved). Solution time of the linear equations increases roughly proportional to the problem size raised to an exponent of about 1.4–1.6 (using iterative solvers) or 3 for direct solvers. In typical, large STARS runs, on the order of 60% of the execution time is spent in the linear equation solver and a further 30% is spent setting up the Jacobian matrices.

2.2 Comparison with Experiments

Computerized Tomography (CT) experiments reported by Izgec et al. (2007) were used to calibrate the numerical model. In these experiments heterogeneous carbonate cores drilled from a carbonate formation were used. Experiments modeled fast near well bore flows (60 ml/min) as well as slow reservoir flows (3 ml/min) at differing temperature (18, 35, and 50°C) and differing orientations (vertical and horizontal). For vertically aligned experiments epoxy coated core plugs of 10.7 cm long and 4.72 cm in diameter as opposed to 7 cm long and 3.81 cm ones in horizontal experiments were used. In all experiments porosity values along the core plugs were measured at the end of each CO_2 injection period using a computerized tomography scanner. Absolute permeability to NaBr brine at differing concentrations (0, 2.5, 5, and 10%) was calculated using Darcy's law. NaBr brine as opposed to NaCl brine was used in the experiments since NaBr brine provided excellent CT number contrast with that of the CO_2 that enabled tracking of porosity changes as a result of calcite dissolution and deposition. Details of the experiments are reported elsewhere (Izgec et al. 2007).

Radial grid block system with $14 \times 25 \times 24$ blocks was used to model the laboratory experiments (Fig. 1). Initial porosities obtained from CT scans were designated to each block corresponding to a slice. The missing porosities in between the slices were distributed using an inverse-distance squared distribution function. Initial permeabilities of each grid were assumed constant. Brooks–Corey CO_2–water relative permeabilities and Brooks–Corey capillary pressures ($\lambda = 0.4$, $P_d = 0.11$ MPa, $S_{wirr} = 0.13$) were used. Note that low pore size distribution index, λ indicates greater heterogeneity.

Calibration of the simulation model was conducted by changing the following parameters: reaction frequencies of the deposition and dissolution reactions, Kozeny–Carman coefficient, reaction rate scaling factor, blockage effect of particles, adsorption rate of CO_2 and initial concentrations of solid phase carbonate and aqueous phase bicarbonate, aqueous phase NaBr. It was observed that matches could be obtained by setting dissolution and deposition reaction frequencies to 3500 and 550 and Kozeny–Carman coefficient to 6.5. For horizontal-oriented experiments the initial concentration of the dissolved bicarbonate (1 g mole/cm^3) was 10 times higher compared to vertical cases. Figures 2 to 4 give the comparison of experimental

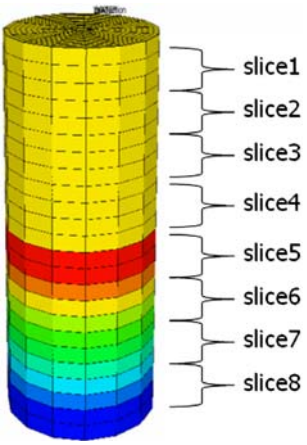

Fig. 1 Distribution of slice porosities in core-scale model

and numerical permeability values for vertical and horizontal oriented heterogeneous and vertical oriented homogenous core plug experiments with varying conditions. For all cases, it was observed that the simulations followed the permeability alteration trend; however, the magnitude of the changes could not be matched exactly. This mismatch could be attributed to the inappropriate representation of the heterogeneous nature of the carbonate core plugs used in the experiments. The results could be further improved by incorporating detailed porosity data. However, it is uncertain whether a simulation model constructed to represent a carbonate can sufficiently capture the essential topological features of these heterogeneous carbonate samples. Nevertheless, results show that composition of the fluids initially present in the core plug and reaction frequencies of the reactions play important roles in fluid–rock–gas interaction leading to changes in rock properties. Xu et al. (2004) reported similar results for sandstones. Blockage effect of calcite and salt particles also play a major role in porosity, thus in permeability alteration trend. Finally, it can be concluded that the calibrated model is capable of reflecting the natural behavior of the CO_2 injection process for all cases and conditions.

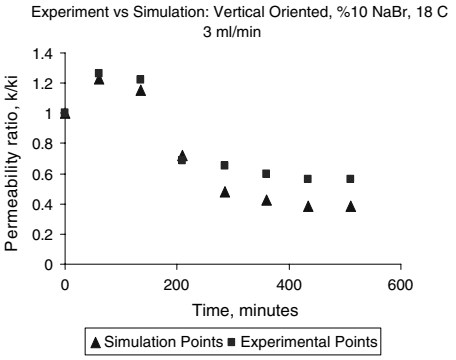

Fig. 2 Calibrated model results for a heterogeneous vertical oriented core plug experiment

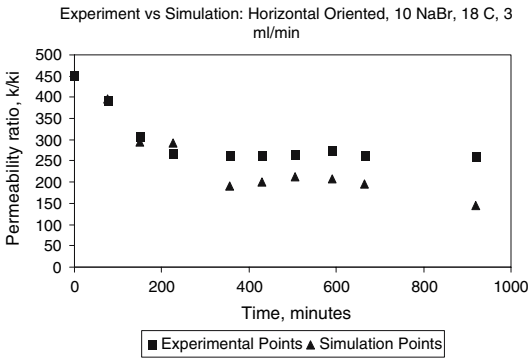

Fig. 3 Calibrated model results for a heterogeneous horizontal oriented core plug experiments

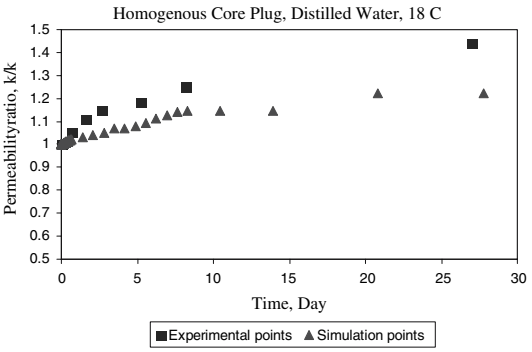

Fig. 4 Calibrated model results for homogenous vertical oriented core plug experiments

Table 1 Simulation parameters

Number of grids	$14 \times 15 \times 24$
Horizontal permeability, md	90
Vertical permeability, md	20
Average effective porosity, %	23.8
Core pressure, kPa	101
Core temperature, °C	18
Injection rate, kg/min	2.507×10^{-3}

2.3 Problem Setup

In order to show the abilities of the model data from one of the matched experiments (Table 1) was used. In this experiment, CO_2 was injected in a continuous manner (3 cc/min) from the bottom of the simulation model. It was observed that chemical reactions occurred preferentially in the center of the core where CO_2 injection is performed (Fig. 5). At this location, the sizes of the grids are relatively smaller than the ones located near the borders. Dissolution and increase in permeability were observed especially at the inlet face of the core plug while at some grid blocks permeability impairment was observed. At the bottom and the top of the core some permeability decreases were also observed. As the injection continued CO_2–rock-brine interaction resulted in various nonuniform dissolution patterns and in some cases re-precipitation and permeability reduction. Thus, it is an unstable dissolution process leading to different dissolution regimes. This unstable dissolution process creates preferential flow patterns so-called wormholes.

Fig. 5 Time dependent (**a**) permeability (md) change, (**b**) CO_2 saturation evolution, (**c**) brine density (kg/cm^3) change, (**d**) adsorbed CO_2 (ppm), and (**e**) concentration of bicarbonate (g-mole/cm^3) (bottom). Model results of experiment 3 at 10, 30, 65, 105, 145, and 180 min (left to right of each image)

A cutting plane at the middle of the core was used to examine the profiles on a vertical plane (Fig. 5). It was observed that injected CO_2 moved toward to top of the core while some amount was dissolved in brine. Figure 5 shows the vertical movement of gaseous CO_2, caused by buoyancy forces, and time-dependent gas saturation distribution. It could be seen that after the vertical movement, free phase gas accumulated at the upper part of the core for a while. Then, CO_2 started to dissolve into water. Thus, gas saturation at the top portion of the core decreased. It is known that dissolution of CO_2 into water increases the density of the brine (Pruess and Xu 2001). Change in water mass density by time observed in the simulation shows that as the CO_2 dissolves in brine, the density of brine increases (Fig. 6). This goes on until CO_2 can not be dissolved any more in the brine. Water density increased with time as free phase gas amount was decreasing. As the mass free phase gas at the upper portion of the core dissolved into brine, density of the fluid increased and started to migrate downwards and replaced by unsaturated brine. Results of core-scale simulation reveals that adsorption of CO_2 is less pronounced compared to other trapping mechanisms. Adsorption of CO_2 takes place where CO_2 is in free gas phase. Figure 5 shows the concentration of bicarbonate ions in brine with time. As seen from this figure solid concentration of the bicarbonate in the core plug continuously increased. This means dissolution takes place at the flow path of the CO_2, especially near the inlet. These results are in accord with aforementioned experimental observations (Izgec et al. 2007).

2.4 Sensitivity Analyses

2.4.1 Chemical Reaction Rate Sensitivity

A sensitivity analysis regarding reaction rates can give some understanding of its impact on the overall geochemical behavior of the system. The results of a sensitivity analysis of the effect of forward reaction (dissolution) and backward reaction (re-precipitation) frequencies of Eq. 6 on change in rock properties are given in Fig. 7 (forward and backward reactions). In this figure, average change of permeability in the entire simulation grid is plotted. These results reveal that as the reaction frequency of forward reaction (dissolution) increases the amount of dissolved particles, the total amount of particles that are blocking the throats increases. This leads to decrease in permeability. Meanwhile dissolution of rock leads to

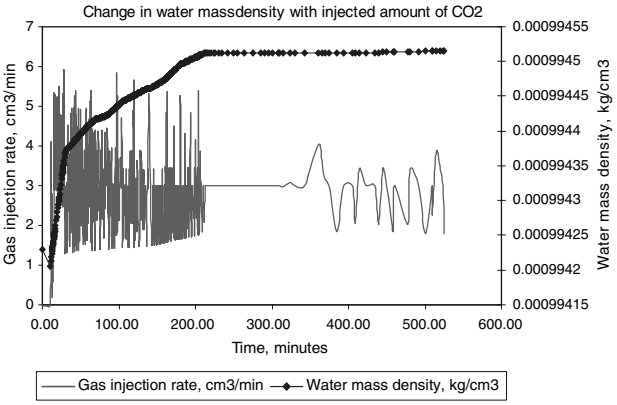

Fig. 6 Time dependent brine density change during the continuous injection of sub-critical CO_2

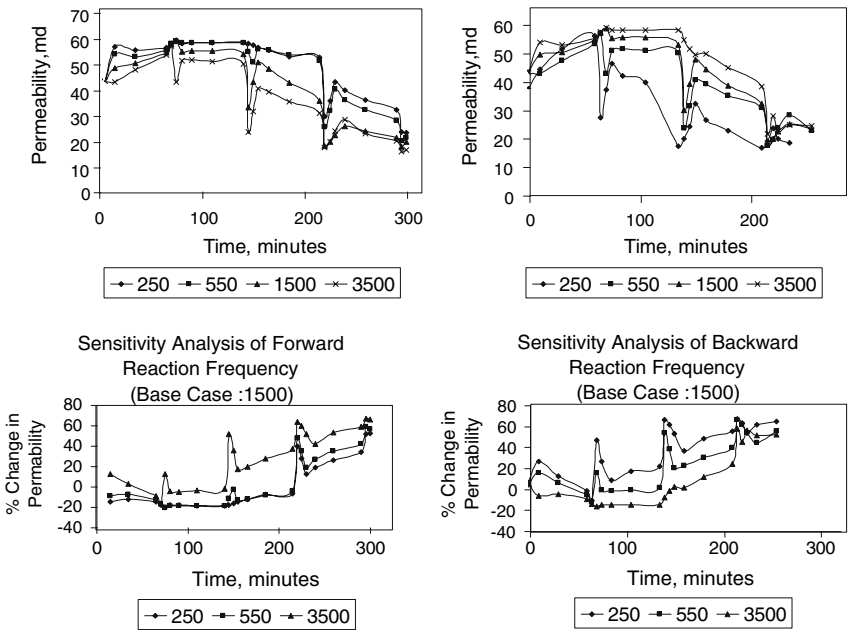

Fig. 7 Sensitivity analysis of forward (left) and backward (right) reaction frequencies

some increase in permeability. But it could be speculated that the effect of particles blocking the pore throats is stronger compared to the permeability increase due to dissolution of rocks. On the other hand, it is observed that increase in backward reaction (re-precipitation), frequency is accompanied with increase in permeability. Backward reaction frequency affects the precipitation rate of insoluble carbonate precipitates. Thus, a decrease in the amount of dissolved particles leads to a decrease in the blockage probability of individual pore throats. During some time-steps, reductions in permeability due to the precipitation of insoluble carbonate precipitates are observed for a number of individual grid blocks. Precipitation of these species leads to decrease in porosity, thus permeability. It could be speculated that the effect of decrease in total amount of particles blocking the pore throats is stronger compared to the permeability reduction due to precipitation and mineralization. The results of sensitivity analysis also reveal that doubling the forward reaction frequency may shift permeability alteration trend about (−) 10% from its previous value for some time-steps. On the other hand, doubling the backward reaction frequency may lead to a 30% increase in permeability of an individual point on permeability alteration trend. As indicated by Xu et al. (2004), CO_2 sequestration by matrix minerals varies considerably with rock type. They further reported that the accumulation of carbonates in the rock matrix lead to a considerable decrease in porosity that in turn adversely affected permeability. As a final remark, the porosity, pore size distribution, and the pore geometry of the rock may also affect the permeability alteration.

2.4.2 Kozeny–Carman Power

Instantaneous permeability values are obtained using these definitions with a Kozeny–Carman type relationship (Eq. 14). Kozeny–Carman type equations were previously used by McCume et al. (1979), Itoi et al. (1987) and Lichtner (1996). Pange and Ziauddin (2005) used a modified

Kozeny–Carman approach to model experimental dissolution patterns observed in carbonates during acidizing process. The application of Eq. 14 with exponents 3, 5, and 12 delineates the possible range of k–ϕ relations (Kühn 2004). The exponent 3 represents clean formations with relatively smooth shaped grains. An exponent of approximately 5 has been determined for anhydrite precipitation found in rock samples of deep geothermal aquifers from Northern Germany. The mineral deposit developed in this case in geological time scales. On the contrary, an exponent of 12 has been determined in core flooding laboratory experiments, representing the technical time scale, where anhydrite dissolved and subsequently precipitated within a temperature front (Bartels et al. 2002). Note that permeability calculated from porosity using Kozeny–Carman type of equation assumes that tortuosity is constant. In practice, however, as carbonic acid dissolves calcite and then precipitates again, the tortuosity should change continuously. For the model developed through this study, permeability is changing continuously because of blockage effects of species produced through chemical interactions among rock–fluid–CO_2. Model calculates instantaneous porosity using void and fluid porosity concepts. The results of a sensitivity analysis of the effect of Kozeny–Carman power, c, on change in rock properties are given in Fig. 8. Results reveal that increasing the Kozeny–Carman power four times may result in up to 43% change in individual points on the permeability alteration trend.

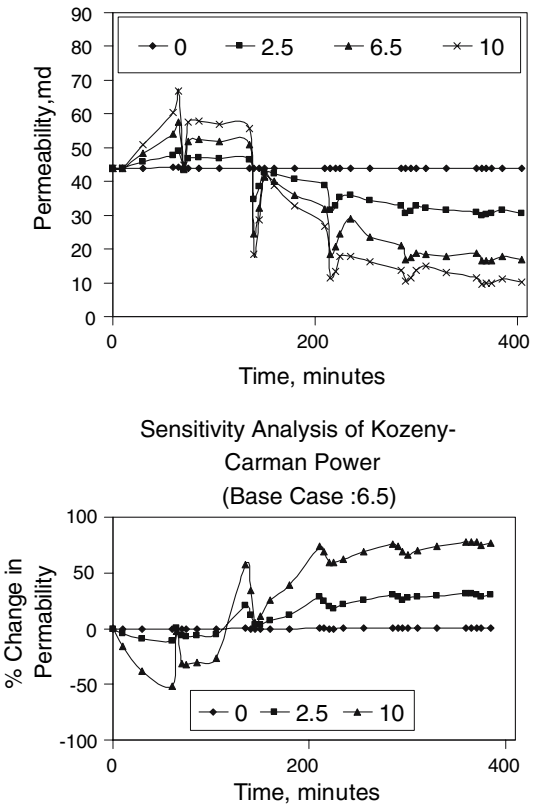

Fig. 8 Sensitivity analysis of Kozeny–Carman power

Table 2 Dependence of reaction or mass transfer rate on permeability

Effective permeability, md	Reaction rate factor, 1/min
10	2.5
20	1
750	0.75
1000	0.5

2.4.3 Blockage Effect of Particles

In computerized tomography monitored CO_2 injection experiments in carbonate core plugs conducted by Izgec et al. (2007), in some parts of the core plugs, a sharp decrease in permeability was observed. They attributed the permeability decrease to the blockage effect of salt and bicarbonate particles. Thus they concluded that salt may precipitate too. The model developed in this study involves the non equilibrium blockage by captured solid (nonfluid) components. Particles may block pore throats through two different mechanisms: bridging and plugging that can be estimated by two empirical relationships (Hibbeler et al. 2003). If pore diameter is less than two times particle diameter, then a bridge will form. If the particle diameter is between 1/3rd and 1/7th the size of the pore diameter then it will plug. Using the relationship that the square root of permeability is approximately equal to pore diameter in microns, plugging range of calcite particles can be calculated. For the heterogeneous carbonate core plugs for which the CO_2 injection experiments were modeled, the pores and throats have small (0.64 μm) to large values (10.65 μm) (Izgec et al. 2007). Thus, the small calcite particles with a particle diameter larger than 0.64 μm could plug the smaller pores along the flow path for all cores except for the homogeneous core plug. Several simulation tests were conducted to achieve an acceptable blockage effect relation in order to calibrate the model. Table 2 summarizes the optimum reaction flow restrictions due to blockage effect of dissolved particles for several permeability values.

2.4.4 Adsorption Rate of CO_2

Adsorption of CO_2 was modeled via compositional dependence specified by the aforementioned Langmuir isotherm coefficients. As seen from the results, absence or presence of adsorption of CO_2 in carbonates has a small effect on permeability alteration trend (Fig. 9). Wang and Thomson (1995) showed that calcite decomposition at high temperatures (i.e., 440 and 560°C) is enhanced when steam is present due to steam's adsorptive properties which are faster and more significant than CO_2 adsorption. They reported that the hypothesis of a quantitative Langmuir type model is compatible with the kinetic data. Zijlma et al. (2000) reported similar results for the influence of H_2O and CO_2 on the reactivity of limestone for the oxidation of NH_3 at high temperatures. Although the temperature range considered in this study is much lower, the results are in accord with the aforementioned studies. Further research is required on this topic in order to generalize the findings.

2.4.5 Initial Concentrations of Species

The effect of initial concentrations of species should be studied to understand and model the process. In Eqs. 1–5, the concentration of CO_2 determines how much bicarbonate will be produced since water and the carbonate amounts in a carbonate reservoir is much larger compared to the concentration of CO_2. The solubility of carbon dioxide in water and hence its

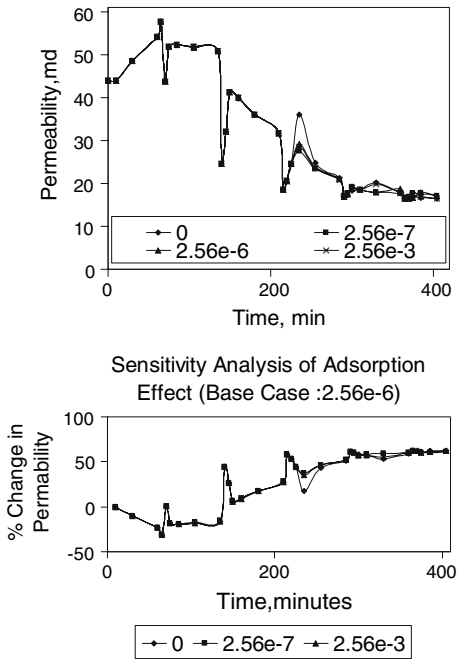

Fig. 9 Sensitivity analysis of CO_2 adsorption

concentration increases with increase in pressure, and decreases with increase in temperature. The solubility of CO_2 is also reduced if the water contains some dissolved solids. Another concept is related to mobilization velocity of particles. Even before the beginning of injection of CO_2, some small particles will already be present in the porous medium. When CO_2 and/or water is injected into the porous medium and the water velocity reaches its mobilization velocity, these particles may move and cause some plugging, hence reducing the permeability of the porous medium. The results of a sensitivity analysis of the effect of initial concentrations of soluble bicarbonate on change in rock properties are given in Fig. 10. Permeability may drastically change if the initial concentration of bicarbonate is high. Thus mobilization of dissolved particles is the effective concept for the permeability alteration behavior.

3 Discussion

Due to numerous uncertainties and approximations such as chemical complexity of injection induced water–CO_2–rock interaction processes, current state-of-the-art numerical models cannot give a complete quantitative prediction of geochemical evolution of CO_2 injection. For example, since the chemical reaction kinetics of heterogeneous reactions are scale and history-dependent, kinetics cannot be reliably quantified. The lack of sufficiently detailed published reaction kinetics data further complicates the problem. In order to avoid adverse effects from CO_2 separating into liquid and gas phases in the injection system, geologic disposal of CO_2 into aquifers would be made at supercritical pressures; however, only a few studies do examine reactions in host rock in response to addition of CO_2 under supercritical conditions. In geochemical modeling studies that incorporate kinetic rate laws

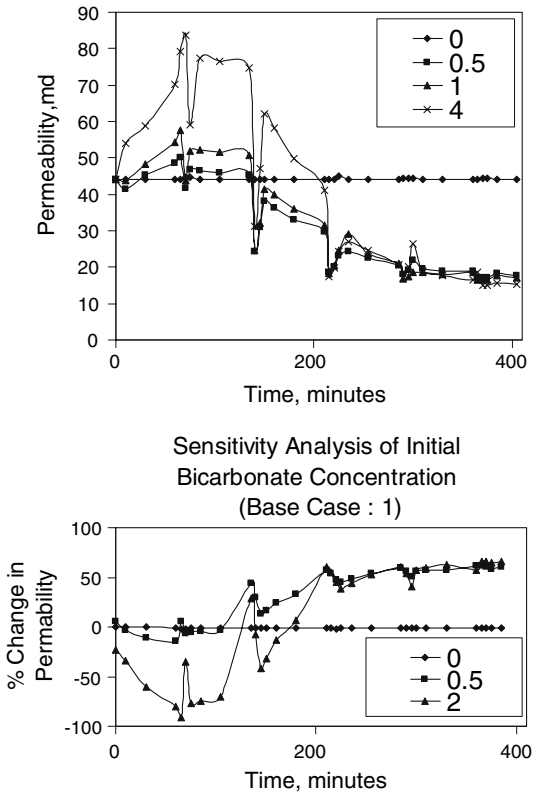

Fig. 10 Sensitivity analysis of initial bicarbonate concentration

(Perkins and Gunter 1995; Gunter et al. 2000) and one study combining experiment and modeling (Gunter et al. 1997), dissolution of silicate minerals in a brine and precipitation of carbonate are reported. In the latter study, however, experiments consisted of month-long batch reactions at 105°C and 90 bars in which no silicate dissolution textures or new major reaction products were observed. With few exceptions (i.e., Gunter et al. 1997; Kaszuba and Janecky 2000; Kaszuba et al. 2001, 2003), there is no published experimental evaluation of geochemical reactions that occur within a supercritical CO_2–brine–aquifer system at reservoir temperature and pressure. For supercritical CO_2 injection at 200°C and 200 bars, Kaszuba et al. (2003) reported that the reaction among supercritical CO_2, brine, and rock exhibits relatively rapid kinetics that are similar to rates measured in systems where gaseous CO_2 is injected. However, numerical modeling is an excellent resource for analyzing and evaluating long term CO_2 sequestration and geochemical performance. A critical evaluation of modeling results can provide useful insight into sequestration mechanisms and controlling geochemical conditions and parameters. Based on the aforementioned observations one could expect that supercritical CO_2 injection will produce similar results to those presented in this study, but further research is required to verify this conclusion.

4 Conclusions

Results of core scale numerical modeling study showed that:

1. STARS can be used for numerical modeling of CO_2 sequestration in deep saline aquifers.
2. Either a permeability improvement or a permeability reduction can be obtained through the injection of CO_2 into carbonate aquifers. The trend of change in rock properties is very case dependent because it is related to distribution of pores, brine composition and as well the thermodynamic conditions.
3. Precipitation process may change permeability and porosity drastically.
4. Composition of the fluids initially present in the formation and reaction frequencies of dissolution and deposition play important roles in fluid–rock–CO_2 interaction leading to change in rock properties. In this regard, adsorption is less significant compared to others.
5. For the short period of simulation time considered in this paper hydrodynamic (free gas phase) and solubility (dissolved) trapping is more pronounced compared to mineral trapping of CO_2 and adsorption of CO_2. Adsorption of CO_2 takes place where CO_2 is in free gas phase.

Acknowledgments This material is based upon work supported by the CNRS (France) and the Scientific and Technical Research Council of Turkey (TUBITAK) under Grant No 102Y154.

References

Allen, D.E., Strazisar, B.R., Soong, Y., Hedges, S.W.: Modeling carbon dioxide sequestration in saline aquifers: significance of elevated pressures and salinities. Fuel Process. Technol. **86**(14–15), 1569–1580 (2005)

Bartels, J., Kühn, M., Schneider, W., Clauser, C., Pape, H., Meyn, V., Lajczak, I.: Core flooding laboratory experiment validates numerical simulation of induced permeability change in reservoir sandstone. Geophys. Res. Lett. **29**(9), (2002). doi:10.1029/2002GL014901

Computer Modeling Group (CMG): CMG STARS User's Guide. Computer Modeling Group LTD., Calgary (2003)

Doughty, C., Pruess, K.: Modeling supercritical carbon dioxide injection in heterogeneous porous media. Vadose Zone J. **3**(3), 837–847 (2004)

Ennis-King, J., Paterson, L.: (2002). Engineering aspects of geological sequestration of carbon dioxide. In: SPE Asia Pacific Oil and Gas Conference and Exhibition, Melbourne, paper SPE 77809

Gunter, W.D., Wiwchar, B., Perkins, E.H.: Aquifer disposal of CO_2-rich greenhouse gases: extension of the time scale of experiment for CO_2-sequestering reactions by geochemical modelling. Mineral. Petrol. **59**, 121–140 (1997)

Gunter, W.D., Perkins, E.H., Hutcheon, I.: Aquifer disposal of acid gases: modelling of water-rock reactions for trapping of acid wastes. Appl. Geochem. **15**, 1085–1095 (2000)

Hibbeler, J., Garcia, T., Chavez, N.: An integrated long term solution for migratory fines damage. In: SPE Latin American and Caribbean Petroleum Engineering Conference, Port of Spain, 27–30 April 2003

Itoi, R., Fukuda, M., Jinno, K., Shimizu, S., Tomita T.: Numerical analysis of the injectivity of wells in the Otake geothermal field, Japan. In: Proceedings of 9th New Zealand Geothermal Workshop, pp 103–108. Geothermal Institute, University of Auckland, Auckland, 4–6 November 1987

Izgec, O., Demiral, B., Bertin, H., Akin, S.: CO2 injection into sline carbonate aquifer formations I: laboratory investigation. Transp. Porous Med. (2007) to appear

Johnson, J.W., Nitao, J.J., Steefel, C.I., Knaus, K.G.: Reactive transport modeling of geologic CO_2 sequestration in saline aquifers: the influence of intra-aquifer shales and the relative effectiveness of structural, solubility, and mineral trapping during prograde and retrograde sequestration. In: Proceedings of 1st Nat. Conf. Carbon Sequestration, Washington (2001)

Kaszuba, J.P., Janecky, D.R.: Experimental hydration and carbonation reactions of MgO: a simple analog for subsurface carbon sequestration processes. Geol. Soc. Am., Abstr. Prog. **32**, A202 (2000)

Kaszuba, J.P., Janecky, D.R., Snow, M.G.: Carbon dioxide reaction processes in a model brine aquifer at 200 C and 200 bars: implications for subsurface carbon sequestration. Geol. Soc. Am. Abstr. Prog. **33**, A232 (2001)

Kaszuba, J.P., Janecky, D.R., Snow, M.G.: Carbon dioxide reaction processes in a model brine aquifer at 200°C and 200 bars: implications for geologic sequestration of carbon.. Appl. Geochem. **18**, 1065–1080 (2003)

Kohse, B.F., Nghiem, L.X., Maeda, H., Ohno, K.: Modelling phase behaviour including the effect of pressure and temperature on asphaltene precipitation. In: SPE Asia Pacific Oil and Gas Conference and Exhibition, Brisbane, Paper SPE 64465, 16–18 October 2000

Korbol, R., Kaddour, A.: Sleipner vest CO_2 disposal-injection of removed CO_2 into the Utsira formation. Energy Convers. Manag. **36**, 509–512 (1995)
Kumar, A., Ozah, R., Noh, M., Pope, G.A., Bryant, S., Sepehrnoori, K., Lake, L.W.: Reservoir simulation of CO_2 storage in deep saline aquifers. SPE J **10**(3), 336–348 (2005)
Kühn, M.: Reactive flow modeling of hydrothermal systems. Lect. Notes Earth Sci. **103**, 209–226 (2004)
Lagneau, V., Pipart, A., Catalette, H.: Reactive transport modelling of CO_2 sequestration in deep saline aquifers. Oil Gas Sci. Technol. Revue De L Institut Francais Du Petrole **60**(2), 231–247 (2005)
Law, D.H., Van der Meer, L.H.G., Gunter, W.D.: Comparison of numerical simulators for greenhouse gas storage in coalbeds, part I: pure carbon dioxide injection. In: Proceedings of 1st Nat. Conf. Carbon Sequestration, Washington (2001)
Lichtner, P.C. (ed.): Reactive transport in porous media (reviews in mineralogy). Mineralogical Society of America, 438 pp (1996)
Matthai, S.K., Belayneh, M.: Fluid flow partitioning between fractures and a permeable rock matrix. Geophys. Res. Lett. **31**(7), Art. No. L07602 (2004)
McCume, C.C., Forgler, H.S., Kline, W.E.: An experiment technique for obtaining permeability-porosity relationship in acidized porous media. Ind. Eng. Chem. Fundam. **18**(2), 188–192 (1979)
McPherson, B.J.O.L., Lichtner, P.C.: CO_2 sequestration in deep aquifers. In: Proceedings of 1st Nat. Conf. Carbon Sequestration. Washington (2001)
Moghadasi, J., Müller-Steinhagen, H., Jamialahmadi, M., Sharif, A.: Model study on the kinetics of oil formation damage due to salt precipitation from injection. J. Petrol. Sci. Eng. **46**(4), 299 (2005)
Omole, O., Osoba, J.S.: Carbon dioxide – dolomite rock interaction during CO_2 flooding process. In: 34th Annual Technical Meeting of the Petroleum Society of CIM, Canada (1983)
Pange, M.K.R., Ziauddin, M.: Two-scale continuum model for simulation of wormholes in carbonate acidization. AIChE J. **51**(12), 3231–3248 (2005)
Perkins, E.H., Gunter, W.D.: Aquifer disposal of CO2-rich greenhouse gasses: modelling of water-rock reaction paths in a siliciclastic aquifer. In: Kharaka, Y.K., Chudaev, O.V. (eds.) Proceedings of 8th Internat. Symp. Water-Rock Interaction, pp. 895–898 (1995)
Pruess, K., Xu, T.: Numerical modeling of aquifer disposal of CO_2. In: SPE/EPA/DOE Exploration and Production Environmental Conference, San Antonio, SPE Paper 83695 (2001)
Pruess, K., Xu, T.F., Apps, J., Garcia, J.: Numerical modeling of aquifer disposal of CO_2. SPE J. **8**(1), 49–60 (2003)
Pruess, K., García, J., Kovscek, T., Oldenburg, C., Rutqvist, J., Steefel, C., Xu, T.: Intercomparison of numerical simulation codes for geologic disposal of CO_2. Lawrence Berkeley National Laboratory Report, LBNL-51813, November 2002
Reichle, D., Houghton, J., Benson, S., Clarke, J., Dahlman, R., Hendrey, G., Herzog, H., Hunter-Cevera, J., Jacobs, G., Judkins, R., Kane, B., Ekmann, J., Ogden, J., Palmisano, A., Socolow, R., Stringer, J., Surles, T., Wolsky, A., Woodward, N., York, M.: Carbon Sequestration Research and Development, Office of Science, Office of Fossil Energy, U.S. Department of Energy (1999)
Sengers, J.M.H.L., Harvey, A.H., Crovetto, R., Gallagher, J.S.: Standard states, reference states and finite-concentration effects in near-critical mixtures with applications to aqueous-solutions. Fluid Phase Equilibria **81**(1–2), 85–107 (1992)
Siu, A.L., Rozon, B.J., Li, Y.K., Nghiem, L.X.: A fully implicit thermal wellbore model for multicomponent fluid flows. SPE California Regional Meeting, Bakersfield, SPE 18777, 5–7 April 1990
Snoeyink, L.W., Jenkins, D.: Water Chemistry. John Wiley & Sons Publications, pp. 85–135 (1980)
Spycher, N., Pruess, K., Ennis-King, J.: CO_2–H_2O mixtures in the geological sequestration of CO_2. I. Assessment and calculation of mutual solubilities from 12 to 100°C and up to 600 bar. Geochim. Cosmochim. Acta **67**(16), 3015–3031 (2003)
Wang, Y., Thomson, W.J.: The effects of steam and carbon-dioxide on calcite decomposition using dynamic X-ray-diffraction. Chem. Eng. Sci. **50**(9), 1373–1382 (1995)
White, S.P., Weir, G.J., Kissling, W.M.: Numerical simulation of CO_2 sequestration in natural CO_2 reservoirs on the Colorado Plateau. In: Proceedings of 1st Nat. Conf. Carbon Sequestration, Washington (2001)
Xu, T.F., Apps, J.A., Pruess, K.: Numerical simulation of CO_2 disposal by mineral trapping in deep aquifers. Appl. Geochem. **19**(6), 917–936 (2004)
Zijlma, G.J., Jensen, A., Johnsson, J.E., van den Bleek, C.M.: The influence of H2O and CO2 on the reactivity of limestone for the oxidation of NH_3. Fuel **79**(12), 1449–1454 (2000)